Leakage loss and group velocity dispersion in air-core photonic bandgap fibers

Kunimasa Saitoh and Masanori Koshiba

Hokkaido University, North 13 West 8, Kita-ku, Sapporo, 060-8628, Japan
ksaitoh@ice.eng.hokudai.ac.jp

Abstract: The wavelength dependence and the structural dependence of leakage loss and group velocity dispersion (GVD) in air-core photonic bandgap fibers (PBGFs) are numerically investigated by using a full-vector finite element method. It is shown that at least seventeen rings of arrays of air holes are required in the cladding region to reduce the leakage losses to a level of 0.1 dB/km in 1.55-μm wavelength range even if using large air holes of the diameter to pitch ratio of 0.9 and that the leakage losses in air-core PBGFs decrease drastically with increasing the hole diameter to pitch ratio. Moreover, it is shown that the waveguide GVD and dispersion slope of air-core PBGFs are much larger than those of conventional silica fibers and that the shape of air-core region greatly affects the leakage losses and the dispersion properties.

OCIS codes: (060.2270) Fiber Characterization; (060.2280) Fiber design and fabrication

References and links

1. J. Broeng, D. Mogilevstev, S.E. Barkou, and A. Bjarklev, "Photonic crystal fibers: A new class of optical waveguides," Opt. Fiber Technol. **5**, 305-330 (1999).
2. T.A. Birks, J.C. Knight, B.J. Mangan, and P.St.J. Russell, "Photonic crystal fibers: An endless variety," IEICE Trans. Electron. **E84-C**, 585-592 (2001).
3. J.C. Knight, T.A. Birks, P.St.J. Russell, and D.M. Atkin, "All-silica single-mode optical fiber with photonic crystal cladding," Opt. Lett. **21**, 1547-1549 (1996).
4. T.A. Birks, J.C. Knight, and P.St.J. Russell, "Endlessly single-mode photonic crystal fiber," Opt. Lett. **22**, 961-963 (1997).
5. J.C. Knight, J. Broeng, T.A. Birks, and P.St.J. Russell, "Photonic band gap guidance in optical fiber," Science **282**, 1476-1478 (1998).
6. R.F. Cregan, B.J. Mangan, J.C. Knight, T.A. Birks, P.St.J. Russell, P.J. Roberts, and D.C. Allan, "Single-mode photonic band gap guidance of light in air," Science **285**, 1537-1539 (1999).
7. J. Broeng, S.E. Barkou, T. Sφndergaard, and A. Bjarklev, "Analysis of air-guiding photonic bandgap fibers," Opt. Lett. **25**, 96-98 (2000).
8. F. Benabid, J.C. Knight, G. Antonopoulos, and P.St.J. Russell, "Stimulated Raman scattering in hydrogen-filled hollow-core photonic crystal fiber," Science **298**, 399-402 (2002).
9. D.G. Ouzouno, F.R. Ahmad, D. Müller, N. Venkataraman, M.T. Gallagher, M.G. Thomas, J. Silcox, K.W. Koch, A.L. Gaeta, "Generation of megawatt optical solitons in hollow-core photonic bang-gap fibers," Science **301**, 1702-1704 (2003).
10. T.P. White, R.C. McPhedran, C.M. de Sterke, L.C. Botten, and M.J. Steel, "Confinement losses in microstructured optical fibers," Opt. Lett. **26**, 1660-1662 (2001).
11. B.T. Kuhlmey, R.C. McPhedran, C.M. de Sterke, P.A. Robinson, G. Renversez, and D. Maystre, "Microstructured optical fibers: where's the edge?," Opt. Express **10**, 1285-1290 (2002), http://www.opticsexpress.org/abstract.cfm?URI=OPEX-10-22-1285
12. D. Ferrarini, L. Vincetti, M. Zoboli, A. Cucinotta, and S. Selleri, "Leakage properties of photonic crystal fibers," Opt. Express **10**, 1314-1319 (2002), http://www.opticsexpress.org/abstract.cfm?URI=OPEX-10-23-1314
13. B. Kuhlmey, G. Renversez, and D. Maystre, "Chromatic dispersion and losses of microstructured optical fibers," Appl. Opt. **42**, 634-639 (2003).

#3147 - $15.00 US Received October 06, 2003; Revised November 04, 2003

14. K. Saitoh, M. Koshiba, T. Hasegawa, and E. Sasaoka, "Chromatic dispersion control in photonic crystal fibers: application to ultra-flattened dispersion," Opt. Express **11**, 843-852 (2003), http://www.opticsexpress.org/abstract.cfm?URI=OPEX-11-8-843
15. G. Renversez, B. Kuhlmey, and R. McPhedran, "Dispersion management with microstructured optical fibers: ultraflattened chromatic dispersion with low losses," Opt. Lett. **28**, 989-991 (2003).
16. K. Saitoh and M. Koshiba, "Confinement losses in air-guiding photonic bandgap fibers," IEEE Photon. Technol. Lett. **15**, 236-238 (2003).
17. N.A. Issa, A. Argyros, M.A. van Eijkelenborg, and J. Zagari, "Identifying hollow waveguide guidance in air-cored microstructured optical fibers," Opt. Express **9**, 996-1001 (2003), http://www.opticsexpress.org/abstract.cfm?URI=OPEX-11-9-996
18. S.G. Johnson, M. Ibanescu, M. Skorobogatiy, O. Weisberg, T.D. Engeness, M. Soljačić, S.A. Jacobs, J.D. Joannopoulos, and Y. Fink, "Low-loss asymptotically single-mode propagation in large-core OmniGuide fibers," Opt. Express **9**, 748-779 (2001), http://www.opticsexpress.org/abstract.cfm?URI=OPEX-9-13-748
19. S.G. Johnson, M. Ibanescu, M.A. Skorobogatiy, O. Weisberg, J.D. Joannopoulos, and Y. Fink, "Perturbation theory for Maxwell's equations with shifting material boundaries," Phys. Rev. E **65**, 066611 (2002).
20. M. Skorobogatiy, S.A. Jacobs, S.G. Johnson, and Y. Fink, "Geometric variations in high index-contrast waveguides, coupled mode theory in curvilinear coordinates," Opt. Express **10**, 1227-1243 (2002), http://www.opticsexpress.org/abstract.cfm?URI=OPEX-10-21-1227
21. T.D. Engeness, M. Ibanescu, S.G. Johnson, O. Weisberg, M. Skorobogatiy, S. Jacobs, and Y. Fink, "Dispersion tailoring and compensation by modal interactions in OmniGuide fibers," Opt. Express **11**, 1175-1196 (2003), http://www.opticsexpress.org/abstract.cfm?URI=OPEX-11-10-1175
22. K. Saitoh and M. Koshiba, "Full-vectorial imaginary-distance beam propagation method based on finite element scheme: Application to photonic crystal fibers," IEEE J. Quantum Electron. **38**, 927-933 (2002).
23. M. Koshiba and Y. Tsuji,"Curvilinear hybrid edge/nodal elements with triangular shape for guided-wave problems," J. Lightwave Technol. **18**, 737-743 (2000).
24. M. Koshiba and K. Saitoh, "Numerical verification of degeneracy in hexagonal photonic crystal fibers," IEEE Photon. Technol. Lett. **13**, 1313-1315 (2001).
25. J.A. Weat, N. Venkataraman, C.M. Smith, and M.T. Gallagher, "Photonic crystal fibers," Proc. European Conf. Opt. Commun., Th.A.2.2 (2001).
26. G. Agrawal, *Nonlinear Fiber Optics*, Academic Press (San Diego, CA), 2dn Edition (1995).

1. Introduction

Optical fibers with silica-air microstructures called photonic crystal fibers (PCFs) [1, 2] have attracted a considerable amount of attention recently, because of their unique properties that are not realised in conventional optical fibers. PCFs, which are also called holey fibers or microstructured fibers, are divided into two different kinds of fibers. The first one guides light by total internal reflection between a solid core and a cladding region with multiple air-holes [3, 4]. On the other hand, the second one uses a perfectly periodic structure exhibiting a photonic bandgap (PBG) effect at the operating wavelength to guide light in a low index core-region [5, 6], which is also called photonic bandgap fiber (PBGF).

Especially, air-core/hollow-core PBGFs [6, 7] have possibilities of extremely low-loss transmission, high-power delivery with low nonlinearity, and many applications such as enhanced Raman scattering [8], soliton transmission [9], and so on. It is very important to know the leakage-loss and dispersion properties of PBGFs for practical applications. A number of studies so far have been made on leakage losses, chromatic dispersion, and imperfection analysis in index-guiding PCFs [10-15], PBGFs [16, 17], and OmniGuide fibers [18-21]. However, the structural dependence of leakage losses and group velocity dispersion (GVD) characteristics in air-core PBGFs with a finite number of air-hole rings has not been reported in the literature.

In this paper, the wavelength dependence and the structural dependence of leakage loss and GVD in air-core PBGFs with a finite number of air-hole rings are numerically investigated by using a full-vector finite element method (FEM). Here, anisotropic perfectly matched layers (PMLs) [22] are incorporated into a full-vector FEM with curvilinear hybrid edge/nodal elements [23] to evaluate leakage losses. It is shown that at least seventeen rings of arrays of air holes are required in the cladding region to reduce the leakage losses to a level of 0.1 dB/km in 1.55-μm wavelength range even if using large air holes of the diameter to pitch ratio of 0.9 and that the leakage losses in air-core PBGFs decrease drastically with

#3147 - $15.00 US Received October 06, 2003; Revised November 04, 2003

increasing the hole diameter to pitch ratio. Moreover, it is shown that the waveguide GVD and dispersion slope of air-core PBGFs are much larger than those of conventional silica fibers and that the shape of air-core region greatly affects the leakage losses and the dispersion properties.

2. Full-vector finite element method formulation

We consider a PCF with finite cross section in the *xy* (transverse) plane and assume that the structure is uniform along the propagation direction (*z* axis), the cross section of which is shown in Fig. 1. In order to enclose the computational domain without affecting the numerical solution and to evaluate leakage losses, anisotropic PMLs [22] are placed before the boundary. From Maxwell's equations the following vector wave equation is derived [22]:

$$\nabla\times([s]^{-1}\nabla\times\boldsymbol{E})-k_0^2n^2[s]\boldsymbol{E}=\boldsymbol{0} \tag{1}$$

where $\boldsymbol{E}$ is the electric field vector, k_0 is the free space wavenumber, n is the refractive index, $[s]$ is the PML matrix, and $[s]^{-1}$ is an inverse matrix of $[s]$. Because of the uniformity of the fiber, we can write the electric field $\boldsymbol{E}$ as

$$\boldsymbol{E}(x,y,z)=\boldsymbol{e}(x,y)\exp(-\gamma z) \tag{2}$$

with

$$\gamma=\alpha+j\beta \tag{3}$$

where γ is the complex propagation constant, α is the attenuation constant, and β is the phase constant, respectively.

In the present formulation curvilinear hybrid edge/nodal elements [23] have been used for accurately modeling curved boundaries [24]. Dividing the fiber cross section into curvilinear hybrid edge/nodal elements and applying the variational finite element procedure, we can obtain the following eigenvalue equation:

$$[K]\{E\}=\gamma^2[M]\{E\} \tag{4}$$

where $\{E\}$ is the discretized electric field vector and the finite element matrices $[K]$ and $[M]$ are given in [22].

The leakage loss, which is also called confinement loss, is an important parameter to design a PCF with a finite number of air holes. In air-core PBGFs with an infinite number of air holes, the light is confined to the air-core region by a full two-dimensional PBG and leakage losses do not occur. In fabricated PBGFs, however, the number of air holes in the cladding is finite, and so the modes of such fibers are inherently leaky. The leakage loss, L_c, is deduced from the value of α as

$$L_c=8.686\alpha \tag{5}$$

in decibels per meter. The waveguide GVD, D_w, is easily calculated from the computed wavelength dependence of the effective index $n_{eff}=\beta/k_0$ as

$$D_w=-\frac{\lambda}{c}\frac{d^2n_{eff}}{d\lambda^2} \tag{6}$$

where λ is the wavelength, c is the velocity of light in a vacuum, and the wavelength dependence of the index of silica is neglected. Of course, the material dispersion should be taken into account to evaluate total wavelength dispersion of PCFs.

#3147 - $15.00 US Received October 06, 2003; Revised November 04, 2003

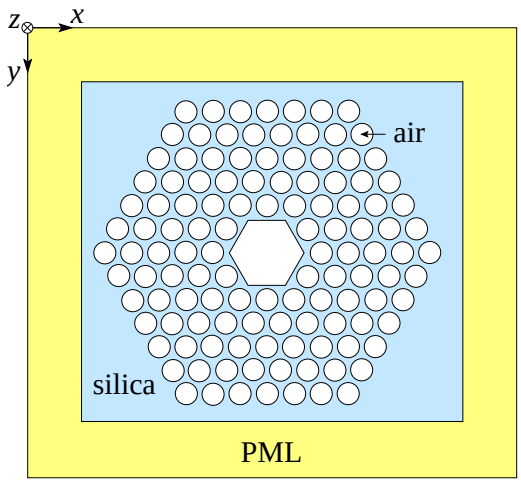

Fig. 1. Photonic crystal fiber with finite cross section.

3. Leakage loss and group velocity dispersion

First, we consider an air-core PBGF [7] with perfectly hexagonal symmetry as shown in Fig. 2, where d is the hole diameter, Λ is the hole pitch (center-to-center distance between the holes), and the background index of silica is 1.45. It is based on the so-called two-dimensional triangular structure and the core region is formed by the removal of seven central holes as illustrated in Fig. 2. Figure 3 shows the modal dispersion curve for hole diameter to pitch ratio $d/\Lambda = 0.9$ as a function of normalized wavelength, λ/Λ, where the number of air-hole rings is ten, the dashed lines are the upper and the lower band-gap edges, and the solid line is the modal dispersion curve for the fundamental mode. The fundamental mode exists inside the PBG region and the lower and higher cutoff wavelengths are, respectively, $\lambda/\Lambda \cong 0.647$ and $\lambda/\Lambda \cong 0.697$. Setting the hole pitch $\Lambda \cong 2.3$ μm and hole diameter to pitch ratio $d/\Lambda = 0.9$, this fiber operates in 1.55-μm wavelength range. Figure 4 shows the intensity profile of the horizontally polarized fundamental mode with $\Lambda = 2.32$ μm and $d/\Lambda = 0.9$ at $\lambda = 1.55$ μm, where the intensity contours are spaced by 1 dB. The field is well confined to the air-core region. However, the number of air holes in the cladding is finite, and so the mode is leaky. Figure 5 shows the wavelength dependence of leakage loss for an air-core PBGF with a finite number of air holes, where $\Lambda = 2.32$ μm, $d/\Lambda = 0.9$, and the number of air-hole rings is taken as a parameter. The leakage loss becomes minimum around the center of PBG and increases as approaching the band edges. Figure 6 shows the leakage loss as a function of number of rings, where $\Lambda = 2.32$ μm, $d/\Lambda = 0.9$, and $\lambda = 1.55$ μm. The leakage loss decreases steadily with increasing number of rings. Note, however, that the rate of reduction in leakage losses is not so fast and that the leakage loss is larger than 10^{-2} dB/m even though the number of rings is ten. In order to realize the leakage loss of 10^{-4} dB/m = 0.1 dB/km in 1.55-μm wavelength range using air-core PBGF with $d/\Lambda = 0.9$, at least seventeen rings are necessary. Figure 7 shows the waveguide GVD of this air-core PBGF with $d/\Lambda = 0.9$ for the fundamental mode, where the number of air-hole rings is taken as a parameter. The GVD is strongly wavelength dependent. It goes from negative values at shorter wavelengths to positive values at longer wavelengths and the dispersion slope is much larger than that of conventional silica fibers. Moreover, the GVD increases rapidly near the upper band edge and it decreases rapidly near the lower band edge, as is pointed out in [25]. We can see that the number of air-hole rings does not affects the GVD around the center of PBG, on the other hand, a change in the number of air-hole rings influences the GVD near the upper and lower band edges.

#3147 - $15.00 US Received October 06, 2003; Revised November 04, 2003

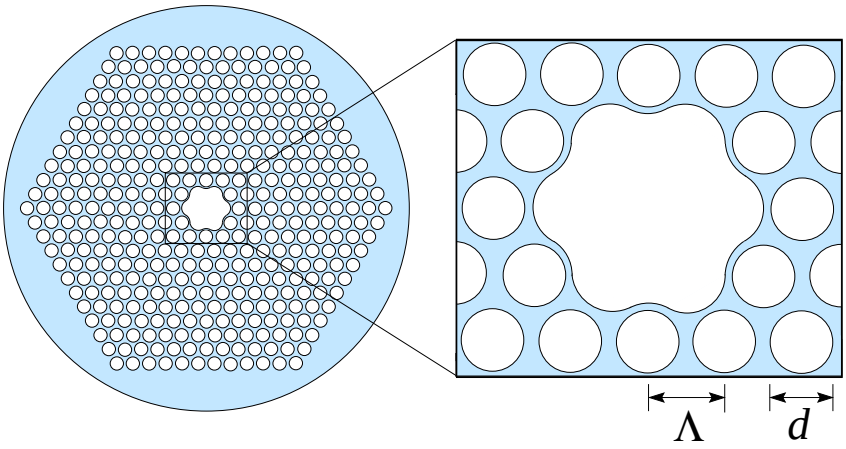

Fig.2. Air-core PBGF with ten rings of arrays of air holes.

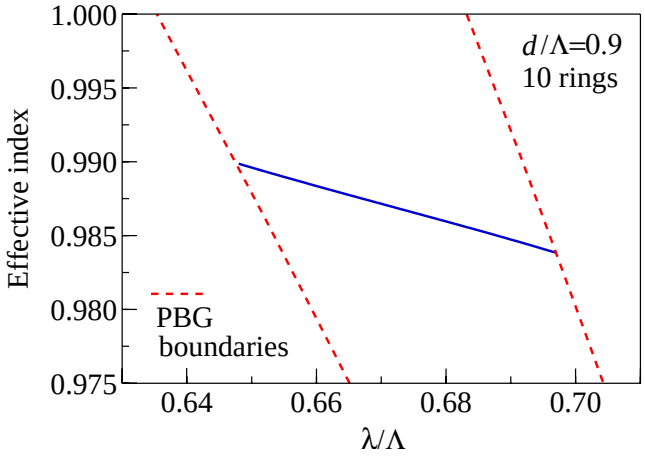

Fig. 3. Modal dispersion curve as a function of normalized wavelength for the air-core PBGF with ten rings of air holes in Fig. 2, where $d/\Lambda = 0.9$.

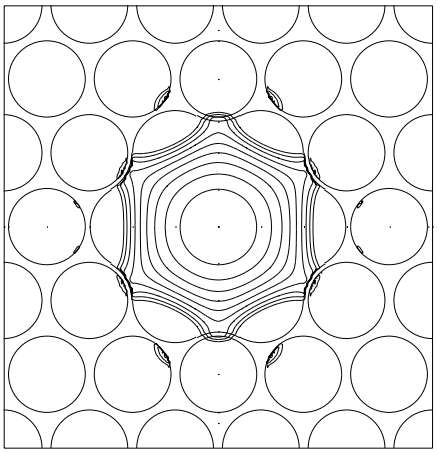

Fig. 4. Intensity profile of horizontally polarized fundamental mode in an air-core PBGF with $d/\Lambda = 0.9$ and $\Lambda = 2.32$ μm at $\lambda = 1.55$ μm, where $|E_x|^2$ is expressed in the intensity contours spaced by 1 dB.

#3147 - $15.00 US
Received October 06, 2003; Revised November 04, 2003

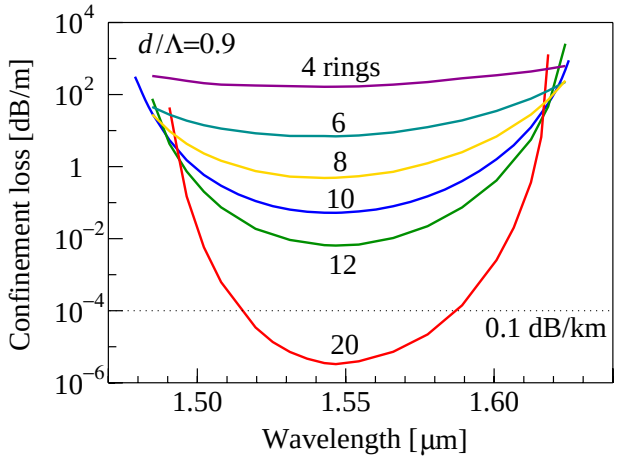

Fig. 5. Leakage loss as a function of wavelength for an air-core PBGF with a finite number of air holes. The hole pitch Λ = 2.32 μm and d/Λ = 0.9.

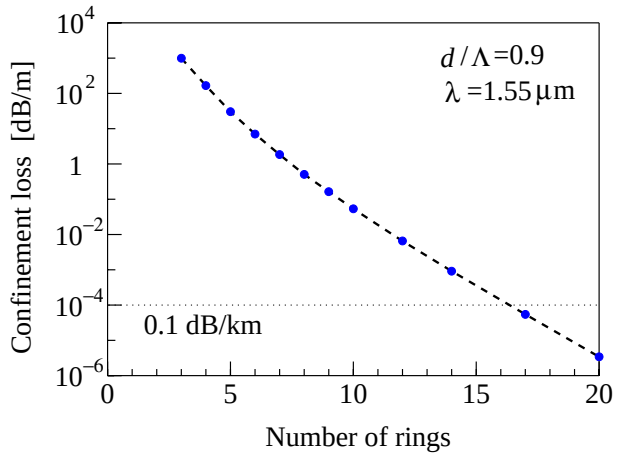

Fig. 6. Leakage loss as a function of the number of rings. The hole pitch Λ = 2.32 μm, d/Λ = 0.9, and λ = 1.55 μm.

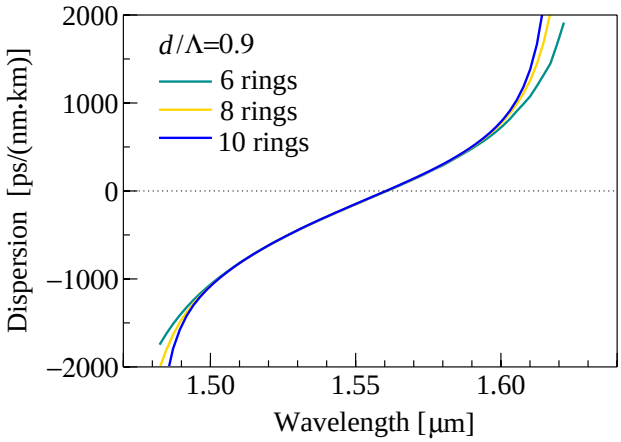

Fig. 7. Waveguide group velocity dispersion of an air-core PBGF with a finite number of air holes. The hole pitch Λ = 2.32 μm and d/Λ = 0.9.

#3147 - $15.00 US
Received October 06, 2003; Revised November 04, 2003

Next, we consider the air-hole diameter dependence of leakage loss and GVD in air-core PBGFs. Figure 8 shows the modal dispersion curves of the fundamental modes for two values of d/Λ = 0.9 and d/Λ = 0.95 as a function of normalized wavelength. The PBGF with d/Λ = 0.95 has the fundamental mode in shorter wavelength range and in wider wavelength range than the PBGF with d/Λ = 0.9. Figure 9 shows the wavelength dependence of the leakage loss for the air-core PBGF with ten rings of air holes in Fig. 2, where the hole diameter to pitch ratio d/Λ is taken as a parameter. The leakage loss decreases drastically with increasing the hole diameter to pitch ratio. Using d/Λ = 0.95 and Λ = 2.74 μm for 10-ring structure, the leakage loss of 0.1 dB/km can be realized in 1.55-μm wavelength range. From these results, we could say that very large value of d/Λ is necessary for reducing the leakage losses in an air-core PBGF with a finite number of air holes in the cladding region. Figure 10 shows the normalized waveguide GVD for the fundamental mode of the air-core PBGF with ten rings of air holes in Fig. 2, where the hole diameter to pitch ratio d/Λ is taken as a parameter. Although an air-core PBGF is expected to be able to exhibit negligible dispersion [7], it has unusual and very large waveguide GVD, especially in the upper and the lower band edge regions. The GVD crosses zero point within the low-loss window. The dispersion slope around the center of PBG for PBGF with larger value of d/Λ is smaller than that for PBGF with smaller value of d/Λ.

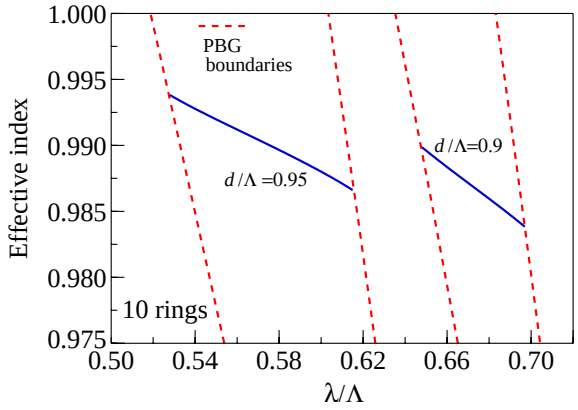

Fig. 8. PBG boundaries and modal dispersion curves of the fundamental modes for two values of d/Λ = 0.9 and d/Λ = 0.95 as a function of normalized wavelength.

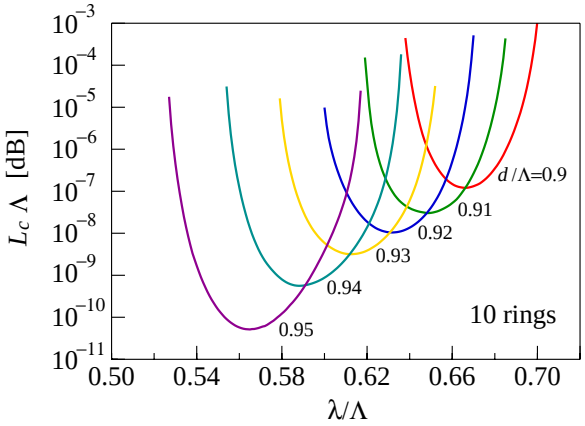

Fig. 9. Normalized leakage loss as a function of the normalized wavelength in an air-core PBGF with ten rings of arrays of air holes. The hole diameter to pitch ratio d/Λ is taken as a parameter.

#3147 - $15.00 US
Received October 06, 2003; Revised November 04, 2003

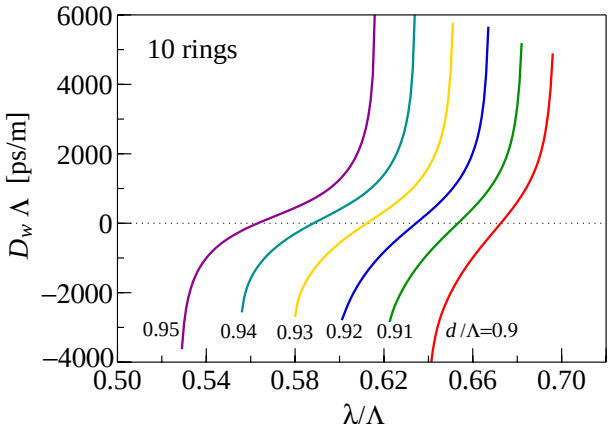

Fig. 10. Normalized waveguide GVD for the fundamental mode of the air-core PBGF with ten rings of air holes in Fig. 2, where the hole diameter to pitch ratio d/Λ is taken as a parameter.

Finally, in order to evaluate the influence of the shape of air-core region on the leakage losses, we consider three types of air-core PBGFs as shown in Fig. 11. Each fiber is formed by the removal of silica around central seven-unit-cell region. The structure shown in Fig. 11(c) is the same as that in Fig. 2. Figure 12 shows the intensity profiles of the horizontally polarized fundamental modes at normalized wavelength $\lambda/\Lambda = 0.67$, where the hole diameter to pitch ratio $d/\Lambda = 0.9$ and the intensity contours are spaced by 1 dB. Each fiber supports the fundamental mode, however, the mode field distributions are different. Figures 13(a) and (b) show, respectively, the modal dispersion curves and the normalized waveguide GVD as a function of normalized wavelength for the three PBGFs in Fig. 11, where $d/\Lambda = 0.9$ and the number of air-hole rings is ten. The guided modes for the three PBGFs exist within almost the same wavelength range, however, the wavelength dependence of the effective index of each PBGF is quite different. Type-3 fiber in Fig. 11(c) has the lowest dispersion slope. Figures 14(a) and (b) show, respectively, the normalized leakage loss and the normalized effective mode area for the three air-core PBGFs in Fig. 11, where $d/\Lambda = 0.9$ and the number of air-hole rings is ten. The effective mode area of the fiber core, A_{eff}, is calculated with [26]

$$A_{eff} = \frac{\left(\iint |\boldsymbol{E}|^2 dxdy\right)^2}{\iint |\boldsymbol{E}|^4 dxdy}. \tag{7}$$

Type-3 PBGF has the lowest leakage loss and the smallest effective mode area among the three PBGFs. These results indicate that the shape of air-core region significantly affects the leakage losses, because the modal dispersion curve is greatly changed by the variation of air-core region.

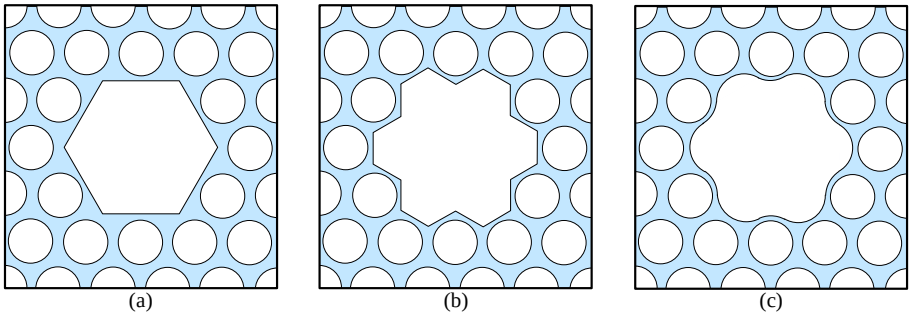

Fig. 11. Schematics of air-core PBGF cross sections for (a) type-1, (b) type-2, and (c) type-3 PBGFs.

#3147 - $15.00 US
Received October 06, 2003; Revised November 04, 2003

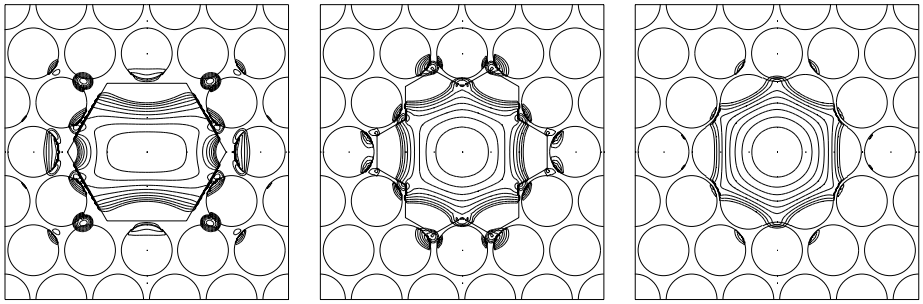

Fig. 12. Intensity profiles of horizontally polarized fundamental modes for air-core PBGFs in Fig. 11, where $d/\Lambda = 0.9$, $\lambda/\Lambda = 0.67$, and $|E_x|^2$ is expressed in the intensity contours spaced by 1 dB.

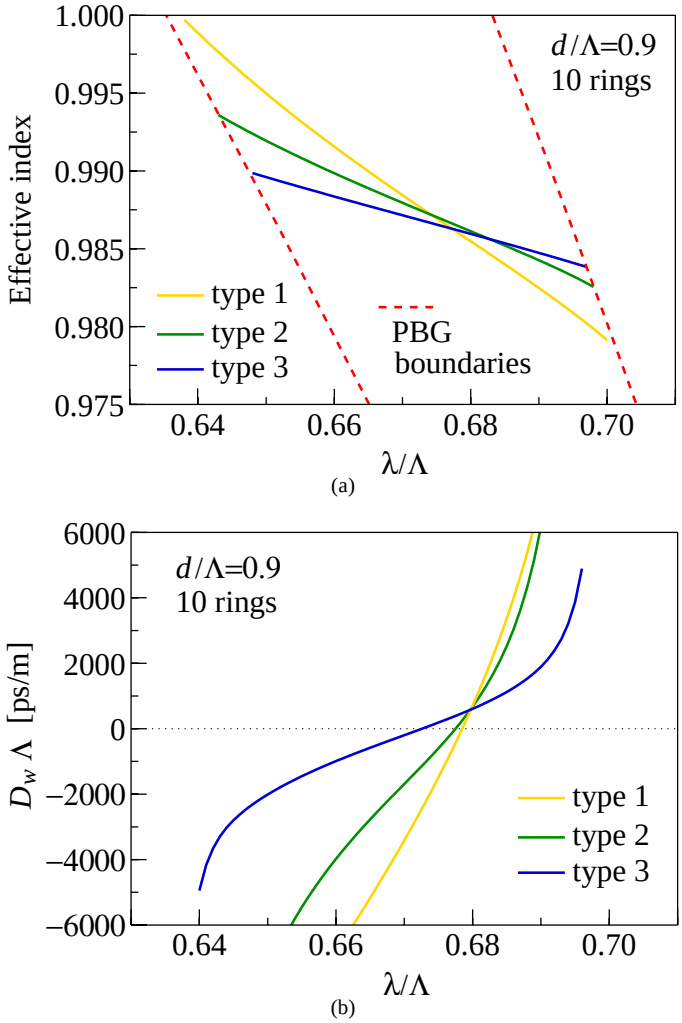

Fig. 13. (a) Modal dispersion curves and (b) normalized waveguide GVD as a function of normalized wavelength for the three types of air-core PBGFs as shown in Fig. 11, where $d/\Lambda = 0.9$ and the number of air-hole rings is ten.

#3147 - $15.00 US
Received October 06, 2003; Revised November 04, 2003

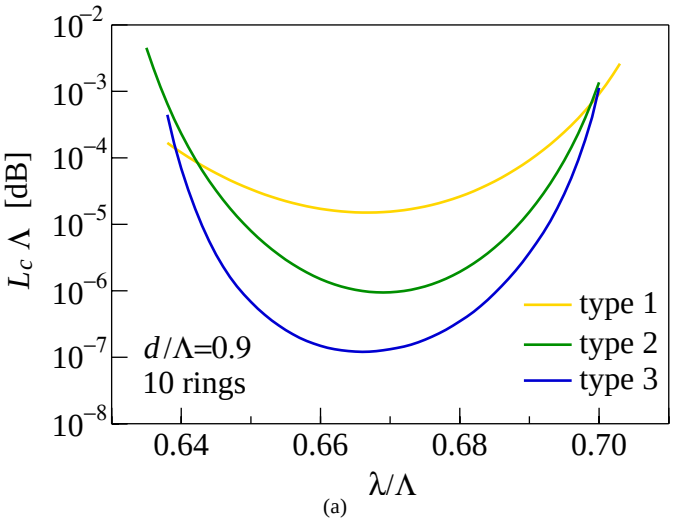

(a)

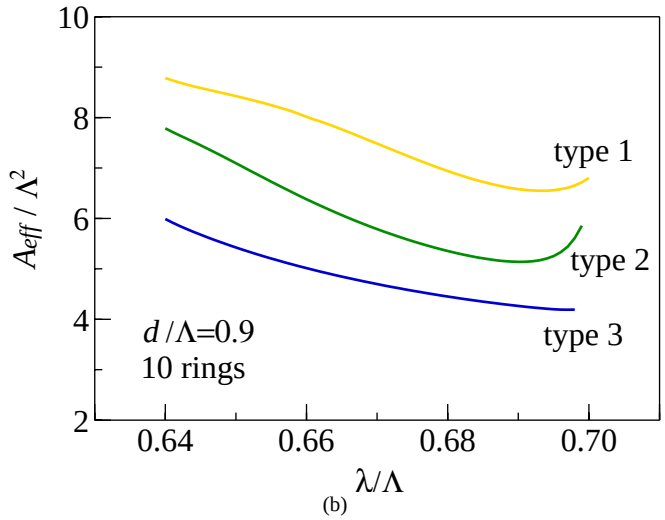

(b)

Fig. 14. (a) Normalized leakage loss and (b) normalized effective mode area as a function of normalized wavelength for the three types of air-core PBGFs as shown in Fig. 11, where d/Λ = 0.9 and the number of air-hole rings is ten.

4. Conclusions

The wavelength dependence and the structural dependence of leakage loss and GVD in air-core PBGFs have been numerically investigated by using a full-vector FEM. It was shown that at least seventeen rings of arrays of air holes are required in the cladding region to reduce the leakage losses to a level of 0.1 dB/km in 1.55-μm wavelength range even if using large air holes of the diameter to pitch ratio of 0.9 and that the leakage losses in air-core PBGFs decrease drastically with increasing the hole diameter to pitch ratio. Moreover, it was shown that the waveguide GVD and dispersion slope of air-core PBGFs are much larger than those of conventional silica fibers and that the shape of air-core region greatly affects the leakage losses and the dispersion properties.

#3147 - $15.00 US
Received October 06, 2003; Revised November 04, 2003